

RSC Advances



This is an *Accepted Manuscript*, which has been through the Royal Society of Chemistry peer review process and has been accepted for publication.

Accepted Manuscripts are published online shortly after acceptance, before technical editing, formatting and proof reading. Using this free service, authors can make their results available to the community, in citable form, before we publish the edited article. This *Accepted Manuscript* will be replaced by the edited, formatted and paginated article as soon as this is available.

You can find more information about *Accepted Manuscripts* in the [Information for Authors](#).

Please note that technical editing may introduce minor changes to the text and/or graphics, which may alter content. The journal's standard [Terms & Conditions](#) and the [Ethical guidelines](#) still apply. In no event shall the Royal Society of Chemistry be held responsible for any errors or omissions in this *Accepted Manuscript* or any consequences arising from the use of any information it contains.

Novel synthesis of Silver/Reduced Graphene Oxide nanocomposite and its high catalytic activity towards hydrogenation of 4-nitrophenol

Received 00th January 20xx,
Accepted 00th January 20xx

DOI: 10.1039/x0xx00000x

Nannan Meng, Shujie Zhang, Yifeng Zhou, Wangyan Nie, and Pengpeng Chen*

www.rsc.org/

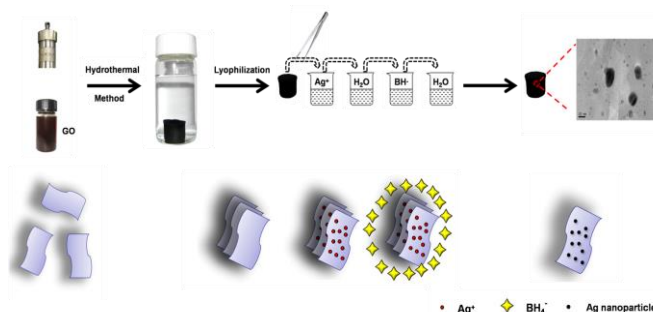
A novel synthesis method was reported for the preparation of silver/reduced graphene oxide (Ag/RGO) nanocomposites via reducing AgNO_3 in a macroscopic RGO aerogel directly through a convenient impregnation process. The as-prepared RGO-supported Ag nanocrystal exhibited high activity in the catalytic hydrogenation of 4-nitrophenol.

Ag has drawn great scientific interest due to its wide range of applications such as in catalysis,¹ surface-enhanced Raman scattering studies,² sensor applications,³ and so on. In particular, the reduction of 4-nitrophenol (4-NP) over Ag nanocatalysts in the presence of NaBH_4 has been intensively investigated for the efficient production of 4-aminophenol (4-AP), which is well known as an important intermediate for the manufacture of analgesic and antipyretic drugs,⁴ photographic developer, corrosion inhibitor, anticorrosion-lubricant, and hair-dyeing agent.⁵ However, due to their high surface energy, Ag nanoparticles easily aggregate, resulting in a marked reduction in their original catalytic activities. Hence, a variety of supports including polymers, metal oxides and carbon materials for Ag nanoparticles anchored on have been extensively reported. For example, recently, we have prepared Ag/poly(styrene-co-hydroxyethyl acrylate) nanoparticles and investigated the influence of molar ratio of DEA/ AgNO_3 on the Raman enhanced performance and catalyze reduction properties of Ag nanoparticles.² Currently, with large surface area and strong mechanical strength, graphene has been successfully employed as a support to stabilize and disperse metal nanoparticles.⁶ These graphene-based nanocomposites with fascinating properties have attracted significant research attention in catalysts and energy applications.⁶ Many approaches have been adopted to fabrication Ag-RGO nanocomposites recently. For example, Ag nanoparticles

were anchored on RGO by a surface modification technique and phase transfer route⁸. Also, Ag-RGO hybrids can be synthesised through reducing silver ions with various reductants, such as N,N-dimethylformamide⁹, hydroquinone¹⁰, and luminal¹¹. Those methods were demonstrated efficient for the inhibition of Ag nanoparticles aggregation and improvement of its catalytic activities, but large amounts of solvent or complicated operations are always involved, which greatly limits their broad application in reality. Therefore, it is essential to search a convenient route for the synthesis of Ag/RGO nanocomposites.

In this work, Ag/RGO nanocomposite was synthesized via a facile impregnation method. The macroscopic RGO aerogel could be obtained via a simple hydrothermal method and its bulk structure was facily impregnated into solutions of AgNO_3 and NaBH_4 successively for formation of Ag/RGO nanocomposite (Scheme. 1.). SEM and TEM showed the aggregation of Ag nanoparticles were inhibited and two kinds of the dominating average size distribution of Ag nanoparticles were 40 ± 5 nm and 5 ± 3 nm, respectively. The obtained Ag/RGO nanocomposite was then used to reduce 4-NP in the present of NaBH_4 and high catalytic activity was demonstrated.

Scheme. 1. Strategy for the synthesis of Ag/RGO nanocomposite.



Anhui Province Key laboratory of Environment-Friendly Polymer Materials, College of Chemistry & Chemical Engineering, Anhui University, Hefei 230601, China
Author to whom correspondence should be addressed:

chenpp@ahu.edu.cn; Tel: 86-551-63861332

† Electronic Supplementary Information (ESI) available: See DOI: 10.1039/x0xx00000x

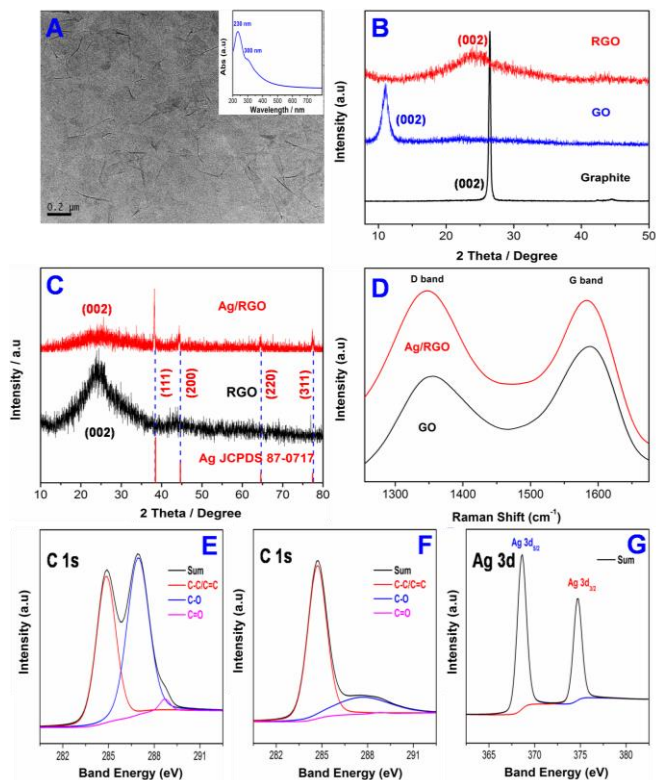


Fig. 1. TEM image (A) and UV-Vis spectroscopy (the insert) of GO; (B) The XRD patterns of the graphite, GO and RGO; (C) The XRD patterns of RGO and Ag/RGO; (D) The Raman spectrums of GO and Ag/RGO. XPS spectra of GO and Ag/RGO nanocomposite [C 1s of GO (E) and Ag/RGO (F); Ag 3d of Ag/RGO (G)]

Graphene oxide (GO), as precursor of RGO, was synthesised as our recently reported method (Supporting Information, SI). Fig. 1A showed the TEM of GO, indicating its typical transparent and two-dimensional morphology. Centred at 230 and 300 nm in UV-Vis absorption peaks of GO (the insert in Fig. 1A) were attributed to the transition of the C=C band and $n-\pi^*$ transition of C=O band, respectively.¹² The FT-IR spectroscopy of GO was shown in Fig. S1. Fig. 1B presented the XRD patterns of graphite, GO and RGO. In Fig. 1B, the XRD pattern of GO displayed a peak at $2\theta=11^\circ$, which was much larger than the d-spacing of graphite at $2\theta=26.5^\circ$. This phenomenon verified graphite had already been oxidized to GO.¹³ After hydrothermal process, $2\theta=11^\circ$ disappeared and a new peak centred at 24.5° , corresponding to the d-spacing of graphene at 0.38 nm appeared, suggesting the reduction of GO to RGO.¹⁴ As shown Fig. 1C, the diffractogram of Ag/RGO showed the peaks of 2θ at 38.1° , 44.3° , 64.5° and 77.4° could be indexed to the (111), (200), (220) and (311) planes of Ag, respectively. Meanwhile, the characteristic diffraction peaks at $2\theta=24.5^\circ$ appeared in Ag/RGO indicating RGO existed in the composite. Notably, no another reflections were presented indicating nanocomposite was purity.¹⁵ The Raman spectra of GO and Ag/RGO nanocomposite were displayed in Fig. 1D. Two marked GO Raman peaks could be seen at 1350 and 1590 cm^{-1} , which were aroused by the D band and G band, respectively.

Both of them were also displayed in the Raman spectrum of Ag/RGO nanocomposite. Compared with that of GO, the intensity ratio of D to G increased significantly suggesting the formation of RGO in Ag/RGO composite.¹⁶ The Raman spectrum of RGO aerogel was also investigated (Fig. S2.). The C1s peak of GO (Fig. 1E) consisted of three main components arising from C-O (hydroxyl and epoxy, 286.5 eV), C-C/C=C (aromatic rings, 284.5 eV) and C=O (carbonyl, 288.5 eV) groups, respectively. After forming the Ag/RGO nanocomposite, C-O and carbonyl groups (Fig. 1F) were markedly reduced.¹⁷ Ag 3d signals displayed in Fig. 1G corresponding to binding energy of Ag supported the result that Ag nanoparticles had been effectively assembled on the surface of graphene nanosheets.¹⁸

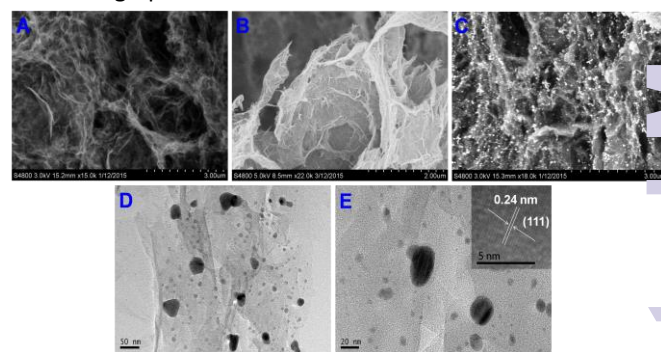
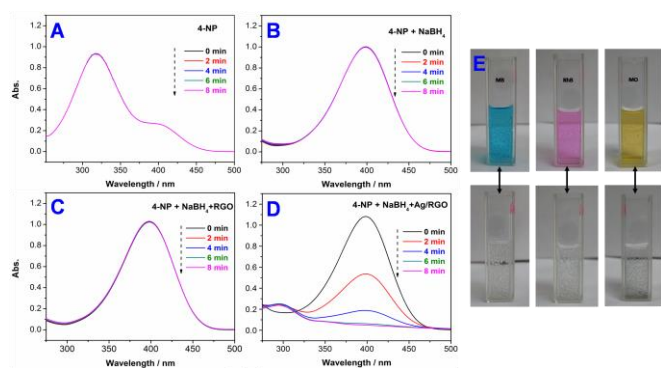


Fig. 2. SEM images of RGO aerogel with (A, B) and without (C) Ag nanoparticles; TEM images of Ag/RGO (D, E) (HR-TEM image of Ag nanoparticle was inserted in E).

The morphology and microstructure of the samples were elucidated by SEM, TEM and HR-TEM. From the SEM image in Fig. 2A, the RGO aerogel sample presented macroporous structure with well-defined interconnected pores and vivid wrinkles (Fig. 2B.). Both the widespread presence of oxygen containing functional groups on RGO verified by XPS and macrostructure with well-defined interconnected pores and wrinkles provided abundant attachment sites for Ag nanoparticles anchored on, thus aggregation of Ag catalysts would be inhibited resulting in its excellent catalytic activity. SEM image of Ag/RGO nanocomposite (Fig. 2C) clearly showed that the Ag particles featured a size of 40 ± 5 nm anchored uniformly on the RGO nanosheets, which was measured from the SEM image (at least 50 particles) as our previously reported.^{2,19,20} However, owing to nanometer-order size (<10 nm), the supported Ag nanocrystals could be hardly observed in the SEM image. The TEM images in Fig. 2D and E revealed that there were plenty of nano-clusters (5 ± 3 nm) distributing on the graphene sheets, which could be aroused by the impregnation treatment.²¹ From the HR-TEM image (the insert of Fig. 2E), the lattice fringe with interplanar spacing of 0.24 nm was well resolved, which could be assigned to the (111) plane of the RGO-supported Ag nanocrystal. The plentiful nano-particles and clusters implied that the RGO-supported Ag excellent candidates as hydrogenation refining materials.

The reduction of 4-NP with NaBH_4 was performed to evaluate the catalytic activity of Ag/RGO nanocomposite. At the beginning, the



intensity of the absorbance remained unchanged in the absence or presence of NaBH_4 after 8 min as shown Fig. 3A and B. Fig. 3C was

Fig. 3. The hydrogenation of 4-NP in the presence of (A) without any other things; (B) NaBH_4 ; (C) NaBH_4 and RGO; and (D) NaBH_4 and Ag/RGO. Photographs of dye solutions with or without Ag/RGO for ca. 10min in the presence of NaBH_4 (E).

the UV-Vis spectra of 4-NP reduction in the presence of NaBH_4 and RGO. The intensity of the absorbance also remained unchanged. However, the addition of Ag/RGO nanocomposite led to a rapid reduction of 4-NP (Fig. 3D.). The absorption of 4-NP at 400 nm decreased, while a new peak simultaneously appeared at 300 nm corresponding to 4-AP.²² Further, in order to efficiently compare the catalytic activities of Ag/RGO and other substrate-supported Ag or Au nanocatalysts. The apparent rate constant (K) was calculated by the following equation based on the pseudo-first-order reaction: $\ln(C_t/C_0) = -Kt$,²³ where K , C_t , and C_0 are apparent rate constant, initial concentration and residual concentration of 4-NP at different intervals, respectively. The apparent rate constant was determined as 0.38952 min^{-1} (Fig. S3.). To compare our result with literature values, the ratio of apparent rate constant K to the total mass of the catalyst ($k=K/m$, where K and m are apparent rate constant and the mass of Ag calculated by ICP, respectively) was calculated. The activity factor for Ag/RGO was $k=2939.3 \text{ min}^{-1} \text{ g}^{-1}$, which is much larger than most of the Ag and Au based catalysts reported previously (Table S1.).²⁴⁻²⁸ The superior catalytic activity of Ag/RGO composite might be caused by the following reasons. On one hand, Ag nanoparticles with sizes from several to tens of nanometers were anchored uniformly on the RGO nanosheets leading to improvement of both numerous active sites and enormous specific area. On the other hand, RGO provided abundant adsorption sites due to π - π stacking between 4-NP and RGO, causing a high concentration of 4-NP near to Ag nanoparticles. Additionally, recycling Ag/RGO composites was also investigated (Fig. S4.). After undergoing three catalysis cycles, no obvious loss of activity was observed, indicating the composites' good durability. Three kinds of dyes, methylene blue (MB), rhodamine (RhB) and methyl orange (MO) were also used to test the ability of Ag/RGO to hydrogenation dyes from water (Fig. 3E). The color of them faded to colorless within 10 min, showing high catalysis efficiencies, too. The results above presented that the Ag/RGO was the better candidate for catalytic application.

Conclusions

Ag/RGO nanocomposite was fabricated via macroscopic RGO aerogel followed by a convenient impregnation reduction process for the first time. The small, highly concentrated, and uniformly dispersed Ag nanoparticles offered a large surface area of active sites for the catalytic reaction. The obtained Ag/RGO nanocomposite was promising for catalysis and sensor applications. The method for preparing Ag/RGO nanocomposite was also considered to be able to obtain some other RGO-based (multi-)metal nanocomposites for fantastic properties.

Acknowledgements

This work was financed by the National Natural Science Foundation of China (Grant No. 51403003), Anhui Provincial Natural Science Foundation (1408085ME86, 1508085QE105), Scientific Research Fund of Anhui Provincial Education Department (KJ2013A014), Startup Foundation for Doctors of Anhui University, Postdoctoral Science Foundation of Anhui Province (01001419), Anhui Provincial Institute of High Performance Rubber Materials and Products and the 211 Project of Anhui University.

Notes and references

- S Kumar, C Selvaraj, LG Scanlon, N Munichandraiah. *Phys Chem Chem Phys*. 2014, 16: 22830-22840.
- ZY Chao, L Wang, LY Song, YF Zhou, WY Nie. *Appl Surf Sci*. 2015, 329: 158-164.
- GG Kumar, KJ Babu, KS Nahm, YJ Hwang. *Rsc Adv*. 2014, 4: 7944.
- Y Du, HL Chen, RZ Chen, NP Xu. *Appl Catal A-Gen*. 2004, 277: 259-264.
- S Saha, A Pal, S Kundu, S Basu, T Pal. *Langmuir*. 2009, 26: 2885-2893.
- HX Chang, HK Wu. *Energ Environ Sci*. 2013, 6: 3483.
- JD Kim, T Palani, MR Kumar, SW Lee, HC Choi. *J Mater Chem*. 2012, 22: 20665.
- S Bai, XP Shen, GX Zhu, Z Xu, YJ Liu. *Carbon*. 2011, 49: 4563-4570.
- YK Yang, CE He, WJ He, LJ Yu, RG Peng, XL Xie, et al. *J Nanopart Res*. 2011, 13: 5571-5581.
- Q Bao, D Zhang, P Qi. *J Colloid Interf Sci*. 2011, 360: 463-470.
- Y He, H Cui. *J Mater Chem*. 2012, 22: 9086.
- I Shown, HC Hsu, YC Chang, CH Lin, Roy PK, Ganguly A, et al. *Nano Lett*. 2014, 14: 6097-6103.
- Etmimi HM, Sanderson RD. *Macromolecules*. 2011, 44: 8504-8515.
- YX Xu, KX Sheng, C Li, GQ Shi. *Acs Nano*. 2010, 4: 4324-4330.
- WH Yuan, YH Gu, L Li. *Appl Surf Sci*. 2012, 261: 753-758.
- P Wang, J Wang, TS Ming, XF Wang, HG Yu, YG Wang, et al. *Acs Appl Mater Inter*. 2013, 5: 2924-2929.
- XT Zhang, ZY Sui, B Xu, SF Yue, TJ Luo, WC Zhan, et al. *J Mater Chem*. 2011, 21: 6494-6497.
- Z Zhang, FG Xu, WS Yang, MY Guo, XD Wang, BL Zhang, et al. *Chem Commun*. 2011, 47: 6440-6442.
- LY Song, WY Nie, YF Zhou. *J Appl Polym Sci*. 2013, 129: 3650-3655.
- SJ Wang, LY Song, PP Chen, YF Zhou, WY Nie. *Colloid and Polymer Science*. 2014, 292, 2465-2473.
- L Delannoy, N El Hassan, A Musi, NN Le To, JM Krafft, C Louis. *J Phys Chem B*. 2006, 110, 22471-22478.
- S Yang, C Nie, HR Liu, HM Liu. *Mater Lett*. 2013, 100: 296-299.

COMMUNICATION

Journal Name

23. Y Feng, NN Feng, GY Zhang and GX Du. CrystEngComm. 2014, 16: 214-222.
24. MH Rashid, TK Mandal. J Phys Chem C. 2007, 111: 16750-16760.
25. S Tang, S Vongehr, X Meng. J Phys Chem C. 2009, 114: 977-982.
26. B Baruah, GJ Gabriel, MJ Akbashev, ME Booher. Langmuir. 2013, 29: 4225-4234.
27. F Ke, L Wang, J Zhu. Nanoscale. 2015, 7: 1201-1208.
28. P Song, LL He, AJ Wang, LP Mei, SX Zhang, JR Chen, et al. J Mater Chem. A. 2015, 3: 5321-5327.

RSC Advances Accepted Manuscript

Graphical Abstract

Novel synthesis of Silver/Reduced Graphene Oxide nanocomposite and its high catalytic activity towards hydrogenation of 4-nitrophenol

Nannan Meng, Shujie Zhang, Yifeng Zhou, Wangyan Nie, and Pengpeng Chen*

Abstract: A novel synthesis method was reported for the preparation of silver/reduced graphene oxide (Ag/RGO) nanocomposites via reducing AgNO_3 in a macroscopic RGO aerogel directly through a convenient impregnation process. The as-prepared RGO-supported Ag nanocrystal exhibited high activity in the catalytic hydrogenation of 4-nitrophenol.

